ISSN 1573-160X, *PHYSICAL OCEANOGRAPHY*, Vol. 31, Iss. 2, pp. 194-207 (2024)

published in *Morskoy Gidrofizicheskiy Zhurnal*, 2024, Vol. 40, Iss. 2, pp. 215–230

Original article

Interannual Salinity Changes in the Upper 1000-Meter Layer of Extratropical Zone in the Northwestern Pacific Ocean under Conditions of the Intensification of Global Hydrological Cycle

I. D. Rostov ✉, E. V. Dmitrieva

V. I. Il'ichev Pacific Oceanological Institute, Far Eastern Branch of Russian Academy of Sciences, Vladivostok, Russian Federation
✉ *rostov@poi.dvo.ru*

Abstract
Purpose. The study is purposed at determining trends and regional features of interannual changes in salinity and salt content in the upper 1000-m layer of extratropical zone in the northwestern Pacific Ocean and at analyzing their possible cause-and-effect relations with large-scale and regional processes in the ocean and atmosphere over the last two decades of the current period of global warming.
Methods and Results. The study is based on NOAA climate data sets on salinity and current velocity in the nodes of the 0.3 × 1º regular grid at 31 levels for 2000–2022 derived from the oceanographic observation system GODAS (NCEP Global Ocean Data Assimilation System), as well as the series both of climate indices from the NOAA websites and routine salinity observations performed at the Rosgidromet coastal hydrometeorological stations. Besides, average monthly ERA5 reanalysis data on precipitation (Reanalysis Data ERA5 monthly 2d Surface) and evaporation from the underlying surface (WHOI OAFlux version3 monthly evapr oaflux) obtained from the NOAA Oceanographic Data Access ERDDAP server were applied. The process of analyzing involved the methods of cluster, correlation and regression analysis, as well as the apparatus of empirical orthogonal functions. The conducted research made it possible to identify and characterize the regional spatial and temporal features of the accelerated changes in salinity and salt content in the upper 1000-m water column of the studied area under conditions of the current warming phase accompanied by the intensification of global and local hydrological cycles. The quantitative characteristics of the noted trends and their statistical significance were assessed.
Conclusions. On the whole, a tendency towards a gradual decrease in average salinity near the sea surface and water desalination in the upper 1000-m layer accompanied by an increase of water heat content in this layer by 3% is observed over the water area under study.

Keywords: northwestern part of the Pacific Ocean, extratropical zone, climate changes, hydrological cycle, salinity, salt content, trends, regional features, climate indices, correlations

Acknowledgments: The study was carried out within the framework of the Comprehensive Interdepartmental Program "Ecological Safety of Kamchatka: Study and Monitoring of Hazardous Natural Phenomena and Human Impacts" (Registration number of NIOKTR 122012700198-9). The authors are grateful to the developers for the opportunity to use the climatic data posted on the NOAA and Rosgidromet websites.

For citation: Rostov, I.D. and Dmitrieva, E.V., 2024. Interannual Salinity Changes in the Upper 1000-Meter Layer of Extratropical Zone in the Northwestern Pacific Ocean under Conditions of the Intensification of Global Hydrological Cycle. *Physical Oceanography*, 31(2), pp. 194-207.

Introduction

Under conditions of accelerating global warming of the atmosphere and ocean [1–3], modern climate changes include intensification of the global water cycle (hydrologic cycle), significant interannual fluctuations in salinity and exacerbation

of spatial contrasts of ocean surface (OSS) and its water column salinity changes from regional to global scale [1, 2, 4, 5–8, 9]. At the same time, the OSS is one of the important components determining ocean circulation and the main indicator of the hydrologic cycle [6]. Large-scale humidification and warming of the atmosphere (as a reaction to an increase in the amount of greenhouse gases and water vapor in the atmosphere) enhance the combined effect of a wide range of processes – components of the water-salt balance – on the formation of OSS anomalies and three-dimensional spatial structures of the salinity field [6, 10]. The intensification of these processes is accompanied by salinity increase in areas with evaporation predominance over precipitation and desalination – in areas with precipitation predominance [1, 3, 11, 12].

Thus, the surface waters of subtropical ocean regions became saltier (~ + 3%) and of tropical and high-latitude regions – fresher (~ −7%) in 1970–2005, which corresponds to an overall increase in freshwater inflow [4, 6] and leads to accelerated halosteric changes in ocean level [8]. As noted before [2, 11], the salinity field reflects a large-scale long-term balance among different components of the surface freshwater flow and the horizontal advection and mixing processes in the ocean. Corresponding response to changes in the hydrologic cycle is characterized by significant spatial and temporal heterogeneity and can be seen in the form of trends in salinity and salt content both on the surface and in the water column of oceans and seas [2, 3, 13]. Globally, the trends of a general salinity increase in the upper ocean layer, which was the greatest one in the maximum salinity area at the 100 m depth, and of decreasing salinity in the 600–1000-m layer of the intermediate minimum salinity were observed in 1970–2005 [3, 6, 14]. The upper 1500-m layer in the Pacific Ocean basin was generally desalinated [3]. At the same time, regional features and three-dimensional spatial structures of salinity and salt content variability of different ocean water column layers under conditions of the current phase of global warming and corresponding changes in the hydrologic cycle remain underestimated and require further analysis.

The present paper aims at determining trends and regional features of interannual changes in salinity and salt content in the upper 1000-m layer of extratropical zone in the northwestern Pacific Ocean and at analyzing their possible cause-and-effect relations with large-scale and regional processes in the ocean and atmosphere in the early 21st century.

Data and methods

Data on salinity and current velocity of the GODAS oceanographic observation assimilation system in grid nodes 0.3° × 1° (https://www.esrl.noaa.gov/psd/data/gridded/data.godas.html) for 2000–2022 and data of regular salinity observations at Rosgidromet coastal hydrometeorological stations (HMSs) and posts off the Kamchatka eastern coast (http://portal.esimo.ru/portal/) were used. The average monthly data concerning precipitation (P) of the ERA5 reanalysis on a grid of 0.25° × 0.25° (http://apdrc.soest.hawaii.edu/erddap/griddap/hawaii_soest_d124_2bb9_c935.html) and evaporation (E) from the underlying surface of WHOI OAFlux version3 on a grid of 1° ×1 ° (http://apdrc.soest.hawaii.edu/erddap/griddap/hawaii_soest_6b5a_df06_3eeb.html?page=1) were also used. The E–P difference value in one-degree grid nodes was calculated based on these data.

The reanalysis data of pressure, wind fields and a series of climate (circulation) indices (CI) [15]: NP, NPGO, PDO, SOI, PTW, IPO, WP, NINO. WEST and WPWP for the same period were also taken. The listed data were obtained from NOAA webpages https://psl.noaa.gov/data/gridded/index.html and https://psl.noaa.gov/data/climateindices/list/. In addition, the composite Kuroshio Extension (KE) index [16] was calculated synthesizing different indicators of low-frequency dynamics of waters in the area of the current continuation (extension) (31–36°N, 140–165°E) closely related to the wind regime characteristics of the northwestern Pacific Ocean.

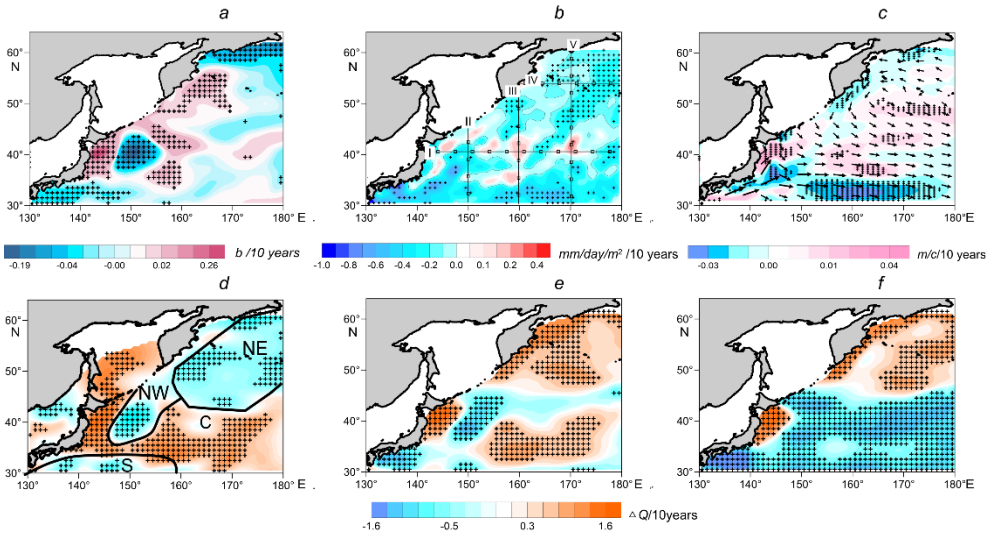

F i g. 1. Trends in mean annual salinity at the 5 m level (*a*), trends in mean annual evaporation-precipitation differences (*b*), currents (arrows) and current velocity trends (highlighted in color) at the 5 m level based on the GODAS data (*c*), trends in the normalized salt content values in the 5–200 m (*d*), 200–460 m (*e*) and 460–950 m layers (*f*) in 2000–2022. Here and in other figures, crosses indicate the areas where the estimates are statistically (95%) significant. Fig. 1, *b* shows the section locations (I, II, III, IV and V) and Fig. 1, *d* shows the selected regions (NE, NW, C and S)

The calculation of statistical parameters and decomposition of anomalous fields of different characteristics into the EOF principal components (PCs) were carried out with unified methods [15]. Additionally, the values of salinity (Qs) and their anomalies (ΔQs) in different depths from the surface down to 1000 meters were calculated based on GODAS data for salinity at 31 levels (uppermost depth of 5 meters) according to the equation provided in [13, p. 3520].

According to the analysis of interannual variability in the salt content of the upper 5–200-m layer, four distinct regions located in different parts of the water area were identified using cluster analysis techniques for three major components of the empirical orthogonal function (EOF): northeastern (NE), northwestern (NW), central (C) and southern (S) (Fig. 1, *d*). Subsequently, the long-term trend in salt content at 31 different levels and in three distinct layers: upper (5–200 m), intermediate (200–460 m) and deep (460–950 m) was determined by averaging the data from the grid within each of these four areas.

Features of interannual spatial and temporal variability of salinity field characteristics

Location of the selected regions (Fig. 1, *d*) is consistent with the position of the structural zones, frontal boundaries and the scheme of main near-surface currents [17, 18] and differs from the zoning of the field of thermal characteristics [19]. The localization of the northeastern region (NE), in which the subarctic water structure is located, corresponds to the location of the Western Subarctic Gyre. The East Kamchatka, Kuril (Oyashio) Currents and the sources of the Subarctic Current can be observed within the boundaries of the northwestern region (NW). The central region (C) position corresponds to the area of mixing of subarctic and subtropical waters in which many isolated mesoscale features and oceanographic structures are formed. The Kuroshio Extension zone is located in the southern region (S) [17, 18].

On average for the region during the period under study, a tendency for a gradual decrease in the average salinity at the surface level of 5 m from a maximum value of 33.82 in 2004 to a minimum of 33.75 in 2018 was observed in the interannual course. According to the data of the Japan Meteorological Agency (https://ds.data.jma.go.jp/tcc/tcc/products/elnino/ensoevents.html), the La Niña phase was expressed in the tropical zone of the Pacific Ocean during autumn 2017 – spring 2018, which was accompanied by an increase in water and air temperatures in the western sector of this zone, the development of ascending convective movements in the atmosphere, its humidification and OSS decrease [1]. Significant trends in the average annual salinity of both signs (up to ±0.2–0.3 over 10 years) at the subsurface level were observed in all selected areas, but mainly in the northern and southwestern parts of the water area under consideration (Fig. 1, *a*). According to observation data at three coastal HMSs located off the Kamchatka southeastern coast (Ossora, Nikolskoye and Petropavlovsk-Kamchatsky), positive trends in interannual changes in salinity have been observed since 1999. Individual areas with maximum positive and negative salinity trends (Fig. 1, *a*) remained well defined throughout the entire water area both in the warm and cold periods of the year.

As noted above, the formation of large-scale spatial and temporal features of the salinity field occurs under changing weather conditions, evaporation, precipitation and other components of the water-salt balance under the influence of advection and vertical mixing processes.

Statistically significant trends in the increase in average annual precipitation were observed in the first decades of the current century (trend 0.3–0.5 mm/day/m^2 over 10 years), mainly in the northern part of the water area, north of 40–45°N, with a maximum value in the cold season (trend 0.5–1.0 mm/day/m^2 over 10 years). Moreover, negative trends in precipitation were expressed in the warm period (from −0.3 to −0.9 mm/day/m^2 over 10 years) in the southwestern part of the water area, south of 40°N. Almost no significant trends in precipitation of both signs were observed in the warm period of the year. It should be noted that similar estimates of precipitation according to https://psl.noaa.gov/data/gridded/data.cmap.html on a 2.5° × 2.5° grid differ somewhat from the above estimates as they are significantly less pronounced by positive trends.

In the interannual course, statistically significant positive trends in average annual evaporation values are expressed within the boundaries of the northeastern

and northwestern regions, negative ones – mainly in the central and southern regions. The spatial distribution of trends in the evaporation-precipitation difference (E–P) demonstrates the predominant nature of precipitation over most of the water area (Fig. 1, *b*) corresponding to global trends in the hydrologic cycle in the middle and high latitudes of the Northern Hemisphere [6, 14], but poorly consistent with the salinity trend distribution (Fig. 1, *a*). As noted earlier [11], in contrast to long-term changes in the characteristics of salinity and humidification of the ocean surface on a global scale [3], trends in spatial changes in the E–P difference in the middle and high latitudes may not coincide with the corresponding regional trends in changes in salinity, since ocean dynamics and local factors can also play a controlling role in changes in the salinity field on the surface and in the ocean water column ensuring its regional balance [14]. One of these factors includes the influence of the processes of ice cover formation and destruction, usually expressed in the seasonal salinity course. At the same time, the analysis did not show any statistically significant linear trends in the long-term distributions of ice cover in the Bering Sea. Its sharp decrease was observed only in recent years after the harsh winter of 2011–2012 [20]. The role of spatial and temporal variability of individual components of the water-salt balance, as well as ocean dynamics (Fig. 1, *c*), in the formation of salinity field anomalies will be considered below based on the correlation and regression analysis methods.

Patterns of spatial features of interannual changes in salt content trends (Qs) of the upper, intermediate and deep layers differ significantly from each other (Fig. 1, *d* – *f*). If in the upper layer the trends of water desalination are expressed only within the boundaries of the northeastern, northwestern and southern regions and salinization trends – in the central region, then this pattern is completely rearranged with increasing depth. Within the intermediate and deep layers of the northwestern Bering Sea and the adjacent waters, extensive areas of increasing salt content are formed and in the deep layer mostly located south of 45°N areas of accelerated water desalination caused by an increase in the fresher water inflow in this latitudinal band are observed [6]. At the same time, in the western part of the Pacific Ocean tropical zone, conditions of precipitation exceeding evaporation prevailed along with trends in increasing the heat and water vapor transfer to temperate latitudes [1, 21, 22], and in the western part of the subtropical gyre, in the Kuroshio region and the northern part of the Philippine Sea, rapid desalination of the upper 800-meter layer in the main halocline region was noted starting from the mid-1990s [23], which can be seen in Fig. 1, *a, d* – *f* in the region of Kuroshio and Kuroshio Extension [17, 18]. The noted trends in the decrease in deep layer salinity and salt content under conditions of intensification of the global hydrological cycle are consistent with the results of other researchers [3, 6, 14]. The spatial distribution patterns of salinity trends in the upper and intermediate layers in the warm and cold periods of the year do not show any noticeable differences.

An interesting feature of the distribution of salinity trends at the surface and the salt content of the entire water column is the localization of the area of their statistically significant positive values in the area located to the southeast of Hokkaido and adjacent to the Sangar Strait (Fig. 1, *a, d* – *f*). As noted before [19], this area with positive trends in heat and salt content was formed as a result of increased water exchange with adjacent areas of the eastern part of the Sea of Japan

(Fig. 1, *c*). Another feature is the area with the maximum negative trends of these values located to the east, with the center in the region of 40–45°N, 150°E, in the zone of convergence of desalinated waters of the Kuril and Subarctic Currents [18]. These features of the distribution of negative trends in salinity and salt content can be observed within the entire 1000-m layer and can be associated with the the wind field [14] effect and the intensification of mesoscale "Kuril" anticyclonic eddies [24] containing cold and desalinated water from the Sea of Okhotsk [19, 25]. The maximum values for the standard deviation of interannual fluctuations in salt content in the 5–200 m layer for the entire region are clearly expressed in the two mentioned regions. The main features of the spatial structure of the trends in the salt content of the upper and intermediate layers (Fig. 1, *d, e*) are in good agreement with the distribution scheme of the coefficients of the first EOF1 mode of decomposition of Qs anomalies, which makes it possible to use the principal component (PC1) of this method of parameterizing Qs fluctuations of these layers to establish correlations with different climate parameters.

Interannual variability of vertical salinity structure of the upper 1000-m layer

According to GODAS data, average profiles of the vertical distribution of salinity for each year and an average profile for the entire 2000–2022 period were obtained within the selected water areas. An analysis of the vertical distribution of trends in average annual salinity at different levels and the principal component PC1 of the EOF for a set of profiles was also carried out (Fig. 2). Analysis of the results obtained revealed a more complex picture compared to that observed in the variability of these characteristics averaged over the entire ocean basin [1, 3, 6, 9, 14] and subject to strong seasonal fluctuations [11].

Smoothed as a result of spatial averaging, the features of the vertical structure of salinity in the area of subarctic water distribution (NE and NW regions) are characterized by a monotonous increase in salinity with depth in the entire upper 1000-meter layer (Fig. 2, *a, d*). Maximum and minimum salinity layers with cores at depths of ~ 200 m and ~ 600–800 m, respectively, are observed in the zone of mixing of subarctic and subtropical waters and the Kuroshio Extension (C and S regions), below the upper halocline (Fig. 2, *g, j*). These layers are identified as subtropical and intermediate waters of the North Pacific Ocean with salinities of ~ 34.4–34.8 and 34.0–34.3 [26]. The PC1(z) curves (Fig. 2, *b*, *e*, *h*, *k*) characterize the amplitude structure of salinity fluctuations at different levels and approximately correspond to the vertical distribution of the range of its changes in the interannual variation (up to 0.11–0.20) and the vertical distribution of salinity trends b(z). The correlation coefficient (R) of PC1(z) and b(z) fluctuations is ±0.9. In general, the principal component PC1(S) in the studied regions accounts for from 53% (S region) to 82–90% (other regions) of the total salinity dispersion at different levels. Features of the vertical structure of salinity trends are formed as a result of the interaction of a wide range of different-scale processes on the ocean surface, advection and vertical mixing. However, in contrast to the characteristics of the vertical amplitude structure of temperature fluctuations in the studied region [19], the maximum values on the PC1(S) curves are observed not only in the upper part of the active layer (Fig. 2, *b, e*), but also in the underlying layers of the water column (Fig. 2, *h, k*).

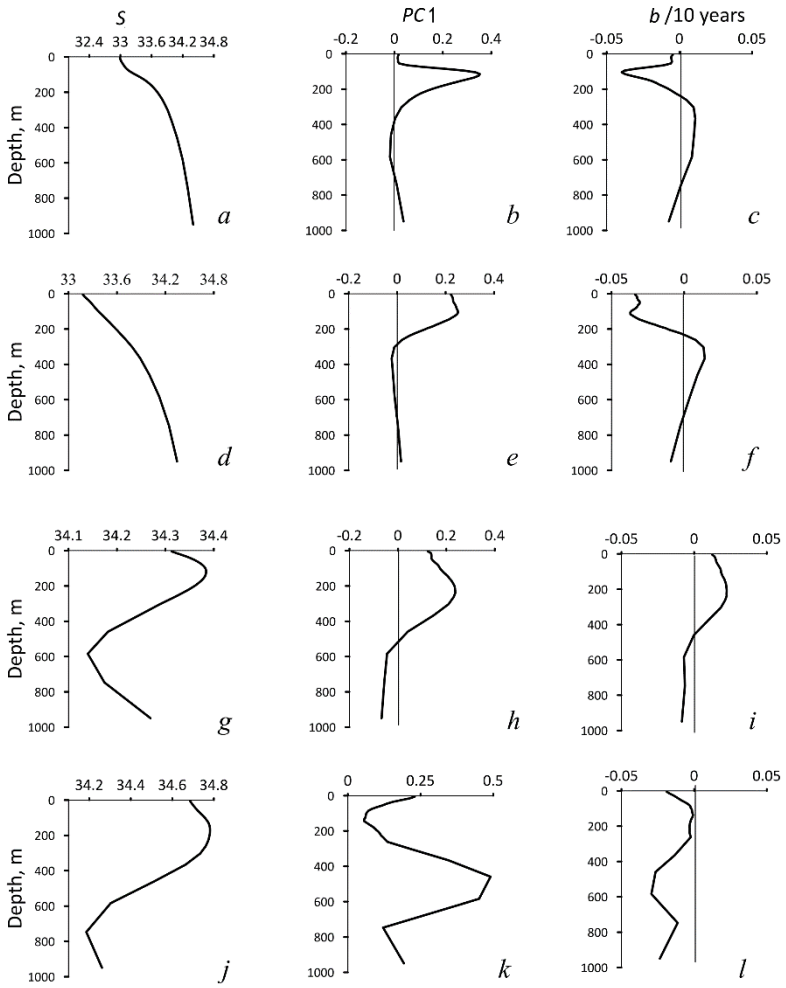

Fig. 2. Generalized curves of vertical distribution of salinity (*a, d, g, j*), principal component PC1 of the EOF of salinity anomalies (*b, e, h, k*) and salinity trend (*b*) at different levels (*c, f, i, l*) for 2000–2022. From top to bottom: the NE, NW, C, S regions according to Fig. 1, *d*

Analysis of interannual trends of statistically significant changes in the vertical structure of salinity showed that maximum freshening had occurred in the upper halocline (−0.04 over 10 years) in the NE and NW regions (Fig. 2, *c, f*) and in the minimum salinity layer (−0.03 for 10 years) in the S region (Fig. 2, *l*). The highest salinity (0.02 over 10 years) was observed in the upper layer of maximum salinity, in the central region (Fig. 2, *i*). These trends are also evident in corresponding changes in estimates of salinity trends in different layers of the studied areas (Table 1; Fig. 1, *d – f*).

Table 1 shows that desalination of the upper and lower layers and salinization of the intermediate layers, which was accompanied by a decrease in the salt content of the entire 1000-meter water column, generally occurred within the entire water area under study for the first decades of the 21st century. As noted earlier [19], an increase by statistically significant 3% was observed in the heat content of this layer water column.

Table 1

Estimates of the linear trend of salt content (Qs, kg·m^{-2}/10 years) in different layers of water column in the identified areas and the entire water area in the 2000–2022 period

Region	Layer boundaries, m			
	5–200	200–460	460–950	5–950
NE	**−3.59**	**1.90**	**1.30**	−0.13
NW	**−5.89**	**2.36**	–0.27	−1.26
C	**3.71**	**3.50**	**−3.03**	**1.39**
S	−0.91	−2.32	**−9.76**	**−4.33**
Average over the entire water area	**−1.67**	**1.36**	**−2.94**	**−1.08**

N o t e. Statistically significant (95%) estimates are highlighted in bold here and in Table 2.

Spatial features of the vertical structure of the water column with different values of desalination and salinization trends are expressed on zonal and meridional sections crossing the water area (Fig. 3).

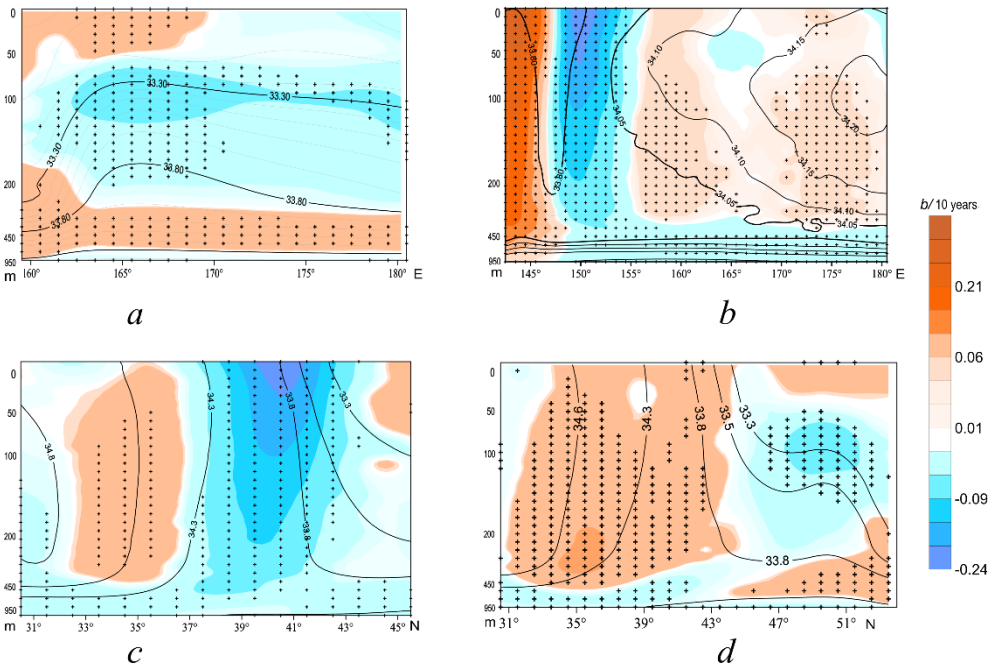

F i g. 3. Combined vertical distribution of salinity (solid lines) and salinity trends (highlighted in color) in zonal sections IV at 53°N (*a*) and I along 40°N (*b*) and at the meridional sections II along 150°E (*c*) and III along 160°E (*d*) in 2000–2022. Section locations are shown in Fig. 1, *b*

The aforementioned features of stratification – layers (water masses) of high and low salinity associated with their sources of origin – are distinguished in all isohaline field sections. The area of maximum statistically significant negative salinity trends can be observed in northern zonal section IV (Fig. 3, *a*) in the 100–400 m layer, in the zone of the greatest horizontal salinity gradients on the western boundary of the North Pacific Gyre and the East Kamchatka Current [11, 18]. Significant positive salinity gradients are expressed in the underlying water column of the entire section

and in the near-surface layer of the western part of this section, which corresponds to Fig. 1. The vertical structure of the salinity field and its trends is completely rearranged in zonal section I (Fig. 1, *b*). One desalination zone with the greatest negative trends in salinity is located in the southern part of the selected NW region (148°–155°E) – the convergence zone of desalinated waters of the Kuril and Subarctic Currents – and covers the entire water column of the upper 1000-meter layer. As noted above, to the west of this zone an area with maximum positive trends in salinity and heat content is pronounced, which is formed as a result of increased water exchange with adjacent areas of the eastern part of the Sea of Japan through the Sangar Strait. Another desalination zone can be observed in the deep layer of 460–1000 m throughout the entire length of section I east of 148°E.

A desalination zone with the greatest negative salinity trends between 37–42°N is also well defined in meridional section II (Fig. 3, *c*) located in the western part of the studied water area. However, the volume of the water column (with the exception of the deep layer of desalinated subarctic waters), in which statistically significant negative salinity trends are observed, gradually decreases, and the volume of the water column with positive trends increases in sections III (Fig. 3, *d*) and V located east of section II.

Correlations of interannual changes in salinity field characteristics with large-scale and regional processes in the ocean and atmosphere

A mutual correlation and regression analysis of interannual variations in time series of salt content and time coefficients (PC1) of the first EOF mode of decomposition of Qs anomalies in the upper and intermediate water column layers with fluctuations in climate indices and other indicators characterizing both the dynamics of the climate system of the atmosphere and ocean and humidification regime in the study area was carried out. Correlation connections in changes in the average annual values of salt content Qs in 5–200 and 200–460 m layers (over the entire region) with different climate variables are most pronounced with the following parameters: NPGO indices (with a time lag of 1 year), KE, WPWP, the second EOF PC2 mode of fluctuations in evaporation-precipitation (E–P) values and the first mode of fluctuations in geopotential anomalies of the isobaric surface AT_{500} – PC1(ΔH_{500}) (Table 2).

The interannual variability of these parameters (except for KE) showed significant trends of different signs during the period under consideration. Maps of the spatial distribution of regression coefficients (Fig. 4) provide a visual representation of the nature of spatial features and the closeness of correlations of changes in salt content and the most important climate parameters in different areas reflecting both regional processes and inter-basin interaction, as well as the remote impact of atmospheric and ocean circulation. These features are in good agreement with the distribution patterns of salt content trends in the upper and intermediate layers (Fig. 1, *d, e*).

The identified relationships characterize the impact of interannual changes in the humidification regime on the ocean surface, advection and vertical mixing, and corresponding regression coefficients are statistically significant over most of the studied water area. These connections are complex and ambiguous and their

nature in the upper (Fig. 4, *a* – *c*) and intermediate (Fig. 4, *d, e*) layers changes significantly with depth. The NPGO index reflects changes in the intensity of the large-scale North Pacific Gyre, is influenced by variability in the position and severity of the atmospheric action centers and the surface wind field associated with sea level pressure fluctuations in the northern Pacific Ocean and has a remote and delayed effect on the Kuroshio-Oyashio current system and thermal conditions of adjacent areas of the marginal seas of the western Pacific Ocean with some phase delay [27].

Table 2

Correlation coefficients of average annual salt content values (Qs) in the 5–200 m and 200–460 m layers with climate indices for different regions for 2000–2022

Regions	Parameter				
	NPGO	KE	WPWP	PC2(E–P)	PC1(ΔH_{500})
5–200 m layer					
NE	0.4	0.2	–0.4	**0.6**	–0.3
NW	**0.7**	–0.4	**0.6**	**0.7**	**–0.6**
C	**–0.7**	0.3	**0.6**	**–0.7**	**0.6**
S	0.4	0.2	–0.3	0.3	**–0.5**
Entire water area	**0.7**	0.0	**–0.5**	**0.8**	**–0.6**
200–460 m layer					
NE	–0.2	**0.6**	**0.5**	–0.2	0.4
NW	–0.1	0.1	0.0	–0.2	0.0
C	–0.4	**0.6**	**0.5**	**–0.5**	0.4
S	0.0	0.3	–0.1	0.1	–0.1
Entire water area	–0.3	**0.7**	0.4	–0.3	0.3

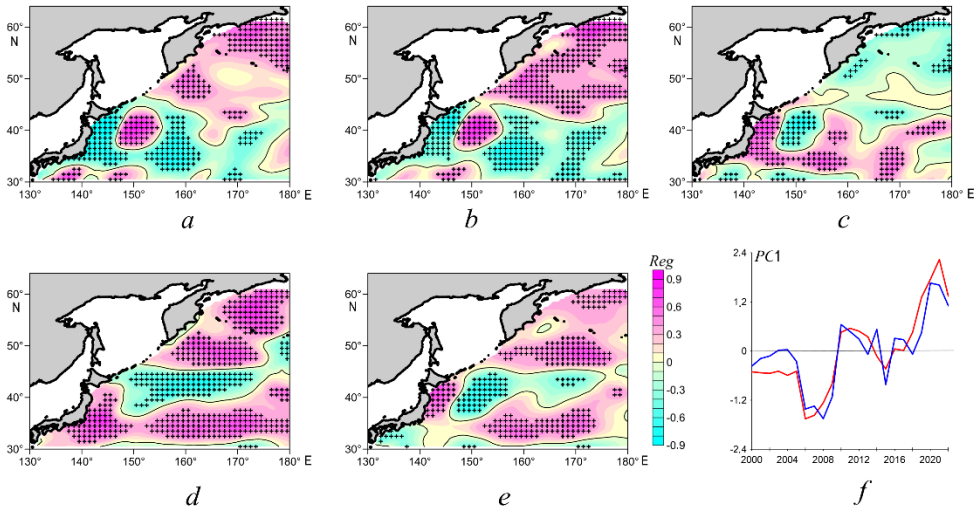

Fig. 4. Linear regression coefficients (Reg) of fluctuations Qs of the average annual salt content anomalies in the 5–200 m layer with NPGO (*a*), PC2(E-P) of evaporation-precipitation difference (*b*) and PC1(ΔH_{500}) (*c*) in 2000–2022. The same is for fluctuations Qs of the 200–600 m layer with KE (*d*) and WPWP (*e*); interannual changes in PC1(Qs) of the intermediate 200–460 m layer (red curve) and the fitting curve of the multiple regression equation with different climate indices (blue curve) (*f*)

The KE index characterizes low-frequency variability of the Kuroshio Extension region – simultaneous changes in its latitudinal position, eastward water transport, level of kinetic energy of eddies and strength of the southern recirculation gyre [16]. The WPWP index characterizes the thermal state of a warm tropical basin located in the western part of the Pacific Ocean equatorial zone [28]. Synchronous connections in interannual fluctuations of these indices are statistically significant (R = 0.5). The PC2(E–P) index characterizes current changes in fresh water flow on the sea surface or humidification regime, and PC1(ΔH_{500}) index shows trends in changes in the pressure field of the isobaric surface geopotential of 500 hPa in the middle troposphere. Fluctuations in these parameters are characterized by negative correlations (R = −0.6) in the warm season.

Variations in the main EOF modes of geopotential anomalies (ΔH_{500}) in the region are closely related to fluctuations in ocean surface temperature, wind field, different climate indices and changes in atmospheric circulation in the region [19]. Thus, their fluctuation connectivity is characterized by correlation coefficient R = – 0.8 with multidirectional trends in interannual changes in PC1(ΔH_{500}) and NPGO. At the same time, the Aleutian Low weakening and strengthening of anticyclonic conditions are accompanied by the NPGO weakening, which can be seen in the current field (Fig. 1, *c*) and in the distribution of corresponding regression coefficients (Fig. 4, *a*).

Note that the value of the explained variance (R^2) of the multiple regression of PC1(Qs) variability of the upper 5–200 m layer and NPGO, PC2(E–P) and PC1(ΔH_{500}) climate variables for 2000–2022 was 58%, i.e., these variables describe satisfactorily the observed Qs changes. For the 200–460 m layer, the R^2 value of multiple regression of these climate indices (Table 2), as well as additional climate indices (NINO.WEST, IPO), was 89% (Fig. 4, *f*). The IPO, WPWP and NINO.WEST indices are commonly used to describe and parameterize the multi-scale variability of thermal conditions in the tropical Pacific Ocean [28, 29].

Conclusion

The performed studies made it possible to identify and characterize regional spatial and temporal features of previously discovered accelerated changes in salinity and salt content in the water column of the upper 1000 m of the studied area under the conditions of the current warming phase accompanied by the intensification of global and local hydrological cycles. Quantitative characteristics of the noted trends and their statistical significance were estimated.

This period was characterized by trends in decreasing precipitation and evaporation from the ocean surface in the southern part of the studied water area with a simultaneous increase in these humidity balance indicators in the north (primarily precipitation – up to 1.0 mm/day/m^2 over 10 years during the cold year period). In general, statistically significant negative trends in the evaporation-precipitation difference were observed throughout the region. In addition, significant changes in different indicators of atmospheric and ocean circulation accompanied by increased water exchange in the extratropical zone of the ocean with adjacent areas were observed at this time, which led to the formation of vast volumes of water columns subject to both desalination and salinization with subsequent transformation of water masses.

Extensive areas of statistically significant S trends of two signs (up to ± 0.2–0.3 over 10 years) were identified in the interannual variation of the average annual salinity at a near-surface level of 5 m in the northern and southwestern parts of the water area under consideration. In general, the water area shows a tendency for a gradual decrease in average salinity values at the surface from a maximum of 33.82 in 2004 to a minimum of 33.75 in 2018.

Variability of the upper 200-m layer salt content Qs demonstrates a tendency towards freshening in the water distribution area of the subarctic structure north of 40–45°N with a trend from −3.6 to −5.9 kg·m^{-2}/10 years and in the Kuroshio Extension strip in the southwestern part of the studied water area (~ −0.9 kg·m^{-2}/10 years). An increasing salt content zone at a rate of ~ 3.7 kg·m^{-2}/10 years is located in the transition zone between these areas. On average, the upper layer waters are desalinated by ~ −1.7 kg·m^{-2}/10 years throughout the entire water area.

The spatial structure of salt content trends is completely rearranged with increasing depth within the intermediate (200–460 m) and deep (460–950 m) layers. On average, salinization of the intermediate layer waters (1.9 kg·m^{-2}/10 years) and desalination of the deep layer (−0.3 kg·m^{-2}/10 years) are observed throughout the entire water area. Moreover, the average salt content of water in the upper 1000-m layer throughout the studied area decreased at a rate of −1.1 kg·m^{-2}/10 years in 2000–2022. According to the authors' earlier estimates, these changes were accompanied by an increase in the heat content of this layer waters by 3%.

In the region as a whole, correlations of changes in the average annual values of salt content Qs in the upper and intermediate 5–200 and 200–460 m layers are most pronounced with the following climate indices and variables: NPGO (with a time lag of 1 year), KE, WPWP, the second EOF mode of fluctuation of evaporation-precipitation (E-P) values and AT_{500} isobaric surface geopotential anomalies.

REFERENCES

1. Intergovernmental Panel on Climate Change (IPCC), 2023. *Climate Change 2021 – The Physical Science Basis: Working Group I Contribution to the Sixth Assessment Report of the Intergovernmental Panel on Climate Change*. Cambridge, United Kingdom: Cambridge University Press, 2391 p. https://doi.org/10.1017/9781009157896
2. Durack, P.J. and Wijffels, S.E., 2010. Fifty-Year Trends in Global Ocean Salinities and Their Relationship to Broad-Scale Warming. *Journal of Climate*, 23(16), pp. 4342-4362. https://doi.org/10.1175/2010JCLI3377.1
3. Skliris, N., Marsh, R., Josey, S.A., Good, S.A., Liu, C. and Allan, R.P., 2014. Salinity Changes in the World Ocean since 1950 in Relation to Changing Surface Freshwater Fluxes. *Climate Dynamics*, 43(3-4), pp. 709-736. https://doi.org/10.1007/s00382-014-2131-7
4. Cheng, L., Trenberth, K.E., Gruber, N., Abraham, J.P., Fasullo, J.T., Li, G., Mann, M.E., Zhao, X. and Zhu, J., 2020. Improved Estimates of Changes in Upper Ocean Salinity and the Hydrological Cycle. *Journal of Climate*, 33(23), pp. 10357-10381. https://doi.org/10.1175/JCLI-D-20-0366.1
5. Durack, P.J., Wijffels, S.E. and Matear, R.J., 2012. Ocean Salinities Reveal Strong Global Water Cycle Intensification during 1950 to 2000. *Science*, 336(6080), pp. 455-458. https://doi.org/10.1126/science.1212222
6. Helm, K.P., Bindoff, N.L. and Church, J.A., 2010. Changes in the Global Hydrological-Cycle Inferred from Ocean Salinity. *Geophysical Research Letters*, 37(18), L18701. https://doi.org/10.1029/2010GL044222

7. Hosoda, S., Suga, T., Shikama, N. and Mizuno, K., 2009. Global Surface Layer Salinity Change Detected by Argo and Its Implication for Hydrological Cycle Intensification. *Journal of Oceanography*, 65(4), pp. 579-586. https://doi.org/10.1007/s10872-009-0049-1

8. Malinin, V.N., 2012. The *Ocean Level: Present and Future*. Saint Petersburg: RSHU Publishers, 260 p. (in Russian).

9. Aretxabaleta, A.L., Smith, K.W. and Kalra, T.S., 2017. Regime Changes in Global Sea Surface Salinity Trend. *Journal of Marine Science and Engineering*, 5(4), 57. https://doi.org/10.3390/jmse5040057

10. Zika, J.D., Skliris, N., Nurser, A.J.G., Josey, S.A., Mudryk, L., Laliberté, F. and Marsh, R., 2015. Maintenance and Broadening of the Ocean's Salinity Distribution by the Water Cycle. *Journal of Climate*, 28(24), pp. 9550-9560. https://doi.org/10.1175/JCLI-D-15-0273.1

11. Liu, Y., Cheng, L., Pan, Y., Abraham, J., Zhang, B., Zhu, J. and Song, J., 2022. Climatological Seasonal Variation of the Upper Ocean Salinity. *International Journal of Climatology*, 42(6), pp. 3477-3498. https://doi.org/10.1002/joc.7428

12. Yu, L., Josey, S.A., Bingham, F.M. and Lee, T., 2020. Intensification of the Global Water Cycle and Evidence from Ocean Salinity: A Synthesis Review. *Annals of the New York Academy of Sciences,* 1472(1), pp. 76-94. https://doi.org/10.1111/nyas.14354

13. Corbett, C.M., Subrahmanyam, B. and Giese, B.S., 2017. A Comparison of Sea Surface Salinity in the Equatorial Pacific Ocean during the 1997-1998, 2012-2013, and 2014-2015 ENSO Events. *Climate Dynamics*, 49(9-10), pp. 3513-3526. https://doi.org/10.1007/s00382-017-3527-y

14. Li, G., Zhang, Y., Xiao, J., Song, X., Abraham, J., Cheng, L. and Zhu, J., 2019. Examining the Salinity Change in the Upper Pacific Ocean during the Argo Period. *Climate Dynamics,* 53(9-11), pp. 6055-6074. https://doi.org/10.1007/s00382-019-04912-z

15. Rostov, I.D., Dmitrieva, E.V. and Rudykh, N.I., 2021. Interannual Variability of Thermal Conditions in the Extratropical Zone of the South Pacific at the Turn of the XX-XXI Centuries. *Physical Oceanography*, 28(6), pp. 612-631. https://doi.org/10.22449/1573-160X-2021-6-612-631

16. Qiu, B., Chen, S., Schneider, N., Oka, E. and Sugimoto, S., 2020. On the Reset of the Wind-Forced Decadal Kuroshio Extension Variability in Late 2017. *Journal of Climate*, 33(24), pp. 10813-10828. https://doi.org/10.1175/JCLI-D-20-0237.1

17. Kuroda, H., Suyama, S., Miyamoto, H., Setou, T. and Nakanowatari, T., 2021. Interdecadal Variability of the Western Subarctic Gyre in the North Pacific Ocean. *Deep Sea Research Part I: Oceanographic Research Papers,* 169, 103461. https://doi.org/10.1016/j.dsr.2020.103461

18. Yasuda, I., 2003. Hydrographic Structure and Variability in the Kuroshio-Oyashio Transition Area. *Journal of Oceanography*, 59(4), pp. 389-402. https://doi.org/10.1023/A:1025580313836

19. Rostov, I.D., Dmitrieva, E.V. and Rudykh, N.I., 2023. Interannual Variability of Thermal Characteristics of the Upper 1000-Meter Layer in the Extratropical Zone of the Northwestern Part of the Pacific Ocean at the Turn of the XX–XXI Centuries. *Physical Oceanography*, 30(2), pp. 141-159.

20. Kattsov, V.M., ed., 2022. [*Third Assessment Report on Climate Changes and Their Consequences on the Territory of the Russian Federation*]. Saint Petersburg: Naukoemkie Technologii, 676 p. (in Russian).

21. Kamae, Y., Mei, W., Xie, S.-P., Naoi, M. and Ueda, H., 2017. Atmospheric Rivers over the Northwestern Pacific: Climatology and Interannual Variability. *Journal of Climate*, 30(15), pp. 5605-5619. https://doi.org/10.1175/jcli-d-16-0875.1

22. Oey, L.-Y. and Chou, S., 2016. Evidence of Rising and Poleward Shift of Storm Surge in Western North Pacific in Recent Decades. *Journal of Geophysical Research: Oceans*, 121(7), pp. 5181-5192. https://doi.org/10.1002/2016JC011777

23. Oka, E., Katsura, S., Inoue, H., Kojima, A., Kitamoto, M., Nakano, T. and Suga, T., 2017. Long-Term Change and Variation of Salinity in the Western North Pacific Subtropical Gyre

Revealed by 50-Year Long Observations along 137° E. *Journal of Oceanography*, 73(4), pp. 479-490. https://doi.org/10.1007/s10872-017-0416-2

24. Yasuda, I., Ito, S.-I., Shimizu, Y., Ichikawa, K., Ueda, K.-I., Honma, T., Uchiyama, M., Watanabe, K., Sunou, N. [et al.], 2000. Cold-Core Anticyclonic Eddies South of the Bussol' Strait in the Northwestern Subarctic Pacific. *Journal of Physical Oceanography*, 30(6), pp. 1137-1157. https://doi.org/10.1175/1520-0485(2000)030<1137:CCAESO>2.0.CO;2

25. Itoh, S. and Yasuda, I., 2010. Characteristics of Mesoscale Eddies in the Kuroshio–Oyashio Extension Region Detected from the Distribution of the Sea Surface Height Anomaly. *Journal of Physical Oceanography,* 40(5), pp. 1018-1034. https://doi.org/10.1175/2009JPO4265.1

27. Ceballos, L.I., Di Lorenzo, E., Hoyos, C.D., Schneider, N. and Taguchi, B., 2009. North Pacific Gyre Oscillation Synchronizes Climate Fluctuations in the Eastern and Western Boundary Systems. *Journal of Climate*, 22(19), pp. 5163-5174. https://doi.org/10.1175/2009JCLI2848.1

28. Cravatte, S., Delcroix, T., Zhang, D., McPhaden, M. and Leloup, J., 2009. Observed Freshening and Warming of the Western Pacific Warm Pool. *Climate Dynamics*, 33(4), pp. 565-589. https://doi.org/10.1007/s00382-009-0526-7

29. Henley, B.J., Gergis, J., Karoly, D.J., Power, S., Kennedy, J. and Folland, C.K., 2015. A Tripole Index for the Interdecadal Pacific Oscillation. *Climate Dynamics*, 45(11-12), pp. 3077-3090. https://doi.org/10.1007/s00382-015-2525-1

Submitted 05.07.2023; approved after review 26.12.2023;
accepted for publication 18.01.2024.

About the authors:

Igor D. Rostov, Head of the Informatics and Ocean Monitoring Laboratory, V.I. Il'ichev Pacific Oceanological Institute, Far Eastern Branch of RAS (3 Baltiyskaya Street, Vladivostok, 690041, Russian Federation), CSc. (Geogr.), **ORCID ID: 0000-0001-5081-7279**, rostov@poi.dvo.ru

Elena V. Dmitrieva, Senior Research Associate, Informatics and Ocean Monitoring Laboratory, V.I. Il'ichev Pacific Oceanological Institute, Far Eastern Branch of RAS (3 Baltiyskaya Street, Vladivostok, 690041, Russian Federation), CSc. (Techn. Sci.), **ORCID ID: 0000-0002-0094-5296**, e_dmitrieva@poi.dvo.ru

Contribution of the authors:

Igor D. Rostov – development of the article structure, processing and analysis of the data, writing the article text

Elena V. Dmitrieva – collection and processing of oceanographic data, calculations, drawing design, text editing

All the authors have read and approved the final manuscript.
The authors declare that they have no conflict of interest.